國 立 交 通 大 學

機 械 工 程 學 系

碩 士 論 文

Realization of High Accuracy FMCW Level Gauge

以 FMCW RADAR 實現高精準度液位量測

研 究 生：羅文祥

指導教授：成維華教授

中華民國九十八年七月

以 FMCW RADAR 實現高精準度液位量測

Realization of High Accuracy FMCW Level Gauge

研　　究　　生：羅文祥　　Student：Wen-Hsiang Lo

指　導　教　授：成維華 博士　　Advisor：Dr. Wei-Hua Chieng

國 立 交 通 大 學

機械工程學系

碩 士 論 文

A thesis

Submitted to Department of Mechanical Engineering

College of Engineering

National Chiao Tung University

in partial Fulfillment of the Requirements

for the Degree of

Master

In

Mechanical Engineering

July 2009

Hsin-chu, Taiwan, Republic of China

中華民國九十八年七月

以 FMCW RADAR 實現高精準度液位量測

研究生:羅文祥　　指導教授:成維華 教授

國立交通大學機械工程學系

中文摘要

儲油槽、油船以及液體儲藏槽都需要液位量測系統對液體進行監控與計量,高精準度液位量測對於各種液位自動控制系統的正常運作以及液體的安全儲藏均有重要的意義。壓力式液位測量系統原理簡單、成本低,但測量精度與應用場合均有一定的限制。超音波液位儀精準度高,但設備複雜且安裝維護麻煩。微波液位量測系統是非接觸性方式,不受液體狀態限制,因此可在高溫、高壓、有毒以及腐蝕性強之液體環境下工作。FMCW 雷達測距系統,具有距離分辨率高、發射功率小等優點。因此我們主要研究 FMCW 液位量測雷達基於 FFT 訊號的高精準度測距原理。

FMCW 雷達的測距誤差受有限長度 FFT 頻譜估測精準度所影響,FFT 過程柵欄效應和頻譜洩漏影響頻率的精準度,而在高精準度要求較高的情況下,直接利用有限長度 FFT 頻譜估測是無法達到精準度的要求,因此本文將提高頻率估測精準度從而提高距離量測精準度。

採取的方法則是利用 FFT 得到 FMCW 雷達差頻訊號峰值的粗略範圍，再利用 Gradient Search Method 訊號處理方式從而實現高精準度之頻譜。

關鍵詞:FMCW 雷達; 柵欄效應; 頻譜洩漏; Gradient Search Method

Realization of High Accuracy FMCW Level Gauge

Student: Wen-Hsiang Lo **Advisor: Dr. Wei-Hua Chieng**

Department of Mechanical Engineering

National Chiao Tung University

Abstract

Oil storages tank, Oil tanker and other process tanks all need liquid level measurement system to monitor and take measurement on liquid. High accuracy measurement of liquid level has great significance on varieties of formal operation on liquid automatic control systems and secure store of liquid. The principle of pressing liquid measure system is uncomplicated and lower-cost, but it has established limitation on measured accuracy and applied fields. The accuracy of liquid level on Ultra-sonic is high, however, the internal parts of equipment is complex and installment and maintainability are troublesome. Measurement liquid level of microwave system is a way of isolation and not to be limited on the state of liquid. Therefore, it is able to perform on the environment of high-temperature, high-pressure, toxic and corrodible liquid. Measurement by FMCW radar system includes the high resolution of measurement range, the lower transmitter power, and so on. For these reason, our research is mainly involved in FMCW level radar which is based on the high accuracy of ranging of FFT signals.

Error in measurement range of FMCW radar is affected from the high accuracy of the estimate of FFT spectrum that is finite length FFT. It will

produce picket fence effects and leakage effects. On the condition that the high accuracy is requested, using the estimate of FFT spectrum directly is unable to achieve the request for the accuracy. Hence, we will increase the accuracy of estimate frequency to increase the accuracy of range estimation. The method we take using FFT to get the rough scope of the peak value on beat frequency signal. And then, use the digital signal processing method to achieve the high accuracy of spectrum.

Key Words: FMCW Radar Picket Fence Effects Leakage Effects Gradient Search Method

致謝

歷經了兩年時光，時光飛逝。感謝成維華老師在學生學習其間的諄諄教誨，不管在做人處事上或是學業研究上的教導，皆讓學生受益良多。

求學期間，感謝呂向斌學長、楊嘉豐學長以及吳秉霖學長的協助指導，使學生得以學習專業領域的知識，並開啟了學習的道路。感謝小隆、之浩 (Dummy)、安鎮和冠今同學們，在求學期間相互的勉勵與扶持，讓我們度過各個知識學習上困難點以及生活上的心靈安慰與實質幫助，讓求學在外的我感受到像家一樣的溫暖。

特別感謝在求學期間父母親在背後默默的支持，不怕艱苦，以及從小教導我該正向的面對問題，好讓我在這研究所期間，碰到問題都能夠順利解決。並感謝我的兄姐們的支持，弟弟能畢業都是因為你們是我的心靈捕手，才能讓我無憂無慮的念書。

最後，感謝我自己，也恭喜我自己畢業了。

Contents

List of Figures

Chapter 1
Introduction

1.1 Thesis Organization

The thesis is organized as follows. First, the basic Frequency Modulation Continuous Wave (FMCW) radar are introduced and applications.

In Chapter 2, include the FMCW radar principle and range and velocity detection.

In Chapter 3, include the FMCW radar system architecture and algorithms.

In Chapter 4, include the raising measuring accuracy algorithm of the FMCW radar.

In Chapter 5, include the simulation and implementation results.

In chapter 6, include the conclusion.

1.2 Research motive

Level measurement is essential in many situations. High accuracy measurement of liquid level system in oil storages tank, Oil tanker and other process tanks all need level measurement system to monitor and take measurement on liquid. High accuracy of level measurement has significance on

varieties of formal operation on liquid automatic control systems and secure store of liquid. The principle of pressing liquid measure system is uncomplicated and lower-cost, but it has established limitation on measured resolution and applied situations. The resolution of level on Ultra-sonic is high. However, the internal part of equipment is complex and installment and maintainability are troublesome. Microwave level measurement system is non-contact with liquid and not to be limited on the state of liquid. Therefore, it is able to perform on the environment of high-temperature, high-pressure, toxic and corrodible liquid. And ranging of FMCW radar system includes the high accuracy of measurement range, the lower of power, and so on. For these reason, our research is mainly involved in FMCW level radar which is based on the high accuracy of ranging of FFT signals.

1.3 History of Radar Development

Although radar did not come into its own until its widespread development and application in World War II, the principle was known and advocated by many now famous scientists of the early 1900s. Table 1-2 provides a chronological list of some highlights and milestones that led to the giant step achieved during World War II.

Since World War II, the use of radar has expanded phenomenally. It has been applied not only to numerous military problems but also to many private and commercial uses. Some of the major postwar developments that stimulated the widespread application and use of radar are as follows:

- High-power klystrons

- Low-noise traveling-wave tube (TWT)
- Parametric amplifiers and masers
- EIO and EIA
- Monopulse
- Over-the-horizon (OTH) radar
- Short pulse techniques
- Synthetic aperture radar
- Phased arrays
- Solid-state devices
- Integrated circuit technology
- Digital computers
- Signal processing
  - Pulse compression
  - MTI and pulsed Doppler
  - Frequency agility
  - Polarization techniques
  - Digital techniques
  - Very-high-speed integrated circuits (VHSIC)

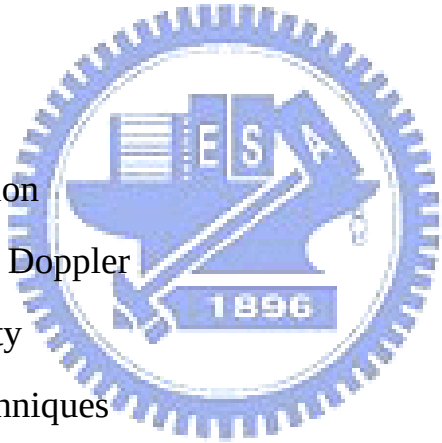

1.4 Application of FMCW Radar

FMCW (Frequency Modulation Continuous Wave) radar is one kind of HF (High Frequency) radar. By using of FMCW radar, we can measure vertical drift velocity (and virtual height) of moving target and measure range of target or object with high resolution.

A range estimation method for FMCW level radar has many advantages. Show the figure 1-1. As a non-contact distance measurement system, that has many advantages surmount other systems in hazardous environment or hard conditions. Owing to its unique features, FMCW radar is often employed where high range measurement resolution and accuracy is demanded.

The surveillance systems become important issues in ITS. In Taiwan, the vehicle detectors are imported till now. The detectors are expensive and unsuitable for the local circumstances. Also, the detectors have high maintenance costs and the foreign companies own the core techniques. As for the microwave-based vehicle detector, the CMOS IC of vehicle detector (first developed in Taiwan) and the antennas developed by ourselves compose the embryo detection system, and the embryo has good performances. Hence, the research team will extend the previous works to promote and improve the capability of microwave-based vehicle detecting systems. Show the figure 1-2.

Car Collision Avoidance System, that is another principal in FMCW radar application field, Is can be one important part of Intelligent Traffic System (ITS), Autonomous Intelligent Cruise Control (AICC) system in safeguard highway traffic security is very important part. In the AICC system, that will use the FMCW radar system to measure range and velocity of the vehicle, and control distance between vehicle and front vehicle by using vehicles' accelerator and the brake. Thus achieves the gold of securable drive.

Therefore, recently for twenty years, FMCW radar brings to people's attention again, and obtains the application in more domains.

Chapter 2
Basic Concepts of FMCW RADAR

One main disadvantage of simple un-modulated CW radar systems is their inability to measure target range. This limitation can be overcome by modulating the CW signals, thus, essentially applying timing mark to the carrier. As mentioned previously, the carrier signal can be modulated in amplitude, frequency, or phase. Pulsed radar is an example of a radar utilizing AM to determine range, Frequency-modulated continuous wave (FMCW) radar techniques are now considered, and multiple-frequency and phase-coded CW radar techniques are discussed in the following subsections.

2.1 Basic principle of FMCW radar

The electronic principle on which radar operates is very similar to the principle of sound-wave reflection. When shouting in the direction of a sound-reflecting object, there comes an echo. According to the speed of sound in air, one can estimate the distance and general direction of the object. The time required for an echo to return can be roughly converted to distance if the speed of sound is known. Radar uses electromagnetic energy in much the same way. The radio-frequency (RF) energy is transmitted to and reflected from the reflecting object. A small portion of the reflected energy returns to the radar set. This returned energy is called an echo, just as it is in sound terminology. Radar sets use the echo to determine the distance of the reflecting object.

$$R_{\max} = \left[\frac{P_t G \mathrm{A}_e \sigma}{(4\pi)^2 P_{\min}} \right]^{\frac{1}{4}} \qquad (2.1)$$

Where $R_{\max}$ = maximum range, m

P_t = transmitted power, watts

G = antenna gain

A_e = antenna effective aperture, m^2

σ = radar cross section, m^2

$P_{\min}$ = minimum detectable signal, watts

Radar system will obey the radar equation in Equation 2.1[1]. It represents the physical dependences and one can access the performance of the radar with the radar equation. First, we assume that electromagnetic waves propagate under ideal conditions. If RF energy is emitted by an isotropic radiator, than the energy propagate uni-formally in all directions. Areas with the same power density therefore form spheres ($A = 4\pi R$) around the radiator. Then in Figure 2-1 it shows that target can be treat as another antenna. RF energy it reflected also propagate uni-formally. And how much it reflect can be replace by a coefficient "σ", Radar Cross Section (RCS). The used to antenna play the role of transmitting and receiving. So antenna gain (G) should be square. And then, when transmitted larger power, the reflection power comes higher. Finally, the system sensitivity will decide the detection of range radar system.

2.2 Pulse and Continuous Wave Radar

After the introduction of radar system basic principle, we will introduce some different kinds of radar system. There are many different technologies for level measurement System such as Ultra-sonic, Infrared and Microwave radar. Microwave radar performs well in every item. So we choose it to implement our anti-collision system. In microwave radar system, there are also several different kinds. Such as pulse radar, FMCW radar and Doppler radar [2]. Pulse radar is popular in war time and has been well developed. Figure 2-2(a) is a simple diagram of how pulse radar works. Generate several RF pulse signals, and find out in which time slot the received signal is. The distance resolution depends on how narrow in time domain the RF pulse is. Relative velocity can be found in the Doppler effecting on RF carrier. The algorithm of pulse radar is quite simple, but implementation of the circuit is much more difficult then FMCW radar.

Figure 2-2(b) is the diagram of FMCW radar. FMCW is the abbreviation of Frequency Modulation Continuous Wave. We add a linear frequency modulation on the center frequency. Figure 2-3, Figure 2-4 is voltage control oscillator (VCO) control voltage versus to time. The time delay between transmitted signal (Tx) and received signal (Rx) will result in a inter-medium frequency (IF) signal. By detecting the IF signal frequency, we can calculate the target distance. Figure 2-3 is the situation without relative velocity and Figure 2-4 is with relative velocity. The inter-medium frequency (IF) signal is the result of distance and relative velocity. Relative velocity causes the Doppler effecting and that will affect the IF frequency higher or lower. Doppler effecting will cause another problem in detection.

Doppler radar is similar to FMCW radar. Since relative velocity will cause some frequency shift. Transmit continuous wave (CW) and detect the frequency difference between transmitted and received signal can get the relative velocity.

2.3 FMCW Radar Range and Velocity Detection

In FMCW radar, the IF frequency is proportional to the distance with target, there is without relative velocity. That can follow FMCW equation [5] to find the distance with target.

$$k = \frac{F_m}{T_m} = \frac{f_b}{t_d} \tag{2.2}$$

$$R = \frac{C \times t_d}{2} \tag{2.3}$$

$$R = \frac{C \times f_b}{2k} \tag{2.4}$$

Where

f_b = beat frequency

t_d = round trip propagation time delay

F_m = frequency deviation

T_m = modulation period

The round trip propagation time t_d is given by

$$t_d = \frac{2R}{c}$$

Where

R= range to target.

C = propagation velocity = $3 \times 10^8 (^{m}/_{s})$.

Velocity detection is according to Doppler effecting. Since Doppler effecting is $f_{Doppler} = \frac{2vf}{c}$ only dependent on the operation frequency and relative velocity. Because IF frequency is the combination of distance and velocity, the control voltage slope rate should be higher enough. Doppler effecting in FMCW radar system will be following below FMCW radar equation.

Doppler Frequency Shift for Moving Target

$$f_d = \frac{2V}{\lambda} = \frac{2Vf}{C} \tag{2.5}$$

And referring to Equation (2.4)

$$f_b = \frac{F_m}{T_m}\frac{4R}{C} \tag{2.6}$$

So

$$f_b = \frac{F_m}{T_m}\frac{4R}{C} + \frac{2Vf}{C} \tag{2.7}$$

For the triangle waveform the upsweep and down-sweep beat frequencies are given by

$$f_b(upsweep) = \frac{-F_m 4R}{T_m C} + \frac{2Vf}{C} \tag{2.8}$$

$$f_b(downsweep) = \frac{F_m 4R}{T_m C} + \frac{2Vf}{C} \tag{2.9}$$

So that range is given by

$$R = \frac{T_m C}{8F_m}\left(f_{b(downsweep)} - f_{b(upsweep)} \right) \tag{2.10}$$

And velocity is given by

$$V = \frac{C}{4f}\left(f_{b(downsweep)} + f_{b(upsweep)} \right) \tag{2.11}$$

Therefore, following these equations, we can find the range and velocity with target.

Chapter 3
FMCW Radar System

A portion of the transmitter signal acts as the reference signal required to produce the beat frequency. It is introduced directly into the receiver via a cable or other direct connection. Ideally, the isolation between transmitting and receiving antennas is made sufficiently large so as to reduce to a negligible level the transmitter leakage signal which arrives at the receiver via the coupling between antennas. The beat frequency is amplified and limited to remove any amplitude fluctuations. The frequency of the amplitude-limited beat note is usually measured with a cycle-counting frequency meter calibrated in distance.

3.1 FMCW Radar System Architecture

Frequency –modulation continuous wave radars are used to measure ranges to targets at a closer distance than pulsed radars can typically operate. Show in the figure 3-1. The same antenna can be employed for both transmit and receive functions when a circulator is used to provide isolation between transmitted and received signals. The heart of the system is a Voltage Controlled Oscillator (VCO) that allows linearized voltage modulation of the output for transmission and acts as the Local Oscillator (LO) of the mixer, generating the intermediate Frequency (IF) from the received echo. Show in the figure 3-2 and figure 3-3.

Constructs a complete microwave radar range detection that should have at least the following several core modules: RF Module, IF Module, Antenna Module, DSP Module, Display /Control Module etc…. Below that will explain

on various module functions, respectively.

A. RF Module

1. SCO (Stable Carrier Oscillator): It mainly uses material quality of the high relative static permittivity to produce a stable carrier frequency signal (f_c) in a series connection feedback loop space. It has the advantage of Phase Noise, Compact Size and frequency stability with temperature etc…. Shown Figure 3-4.

2. FMO/FMS (Frequency Modulate Oscillator/Frequency Modulate Synthesizer): It mainly produces a frequency modulation (FM) signal f_{fm}. That produces the intermediate frequency signal must the quite linearity. Otherwise that will affect the correct obtained of beat frequency signal, creates the error of measurement range.

3. Coupling Filter: It is mainly the radio-frequency signal section which the filter interception needs. ($f_c + f_{fm}$, upside Band).

4. Power Divider: After It will modulate the radio-frequency signal($f_c + f_{fm}$) divides into two groups, one uses as the transmitted, and the other one will provide the receiving end the local oscillations signal(Lo, Local oscillator) to intercept beat frequency signal.

5. Mixer: After it mainly intercept the receive echo and the local oscillations signal which mix beat frequency signal (IF).

6. Low Noise Amplifier (LNA).: It mainly enlarge the radio frequency signal with low noise.

7. Double Side Band Mixer: It mainly does the Stable Carrier Oscillator (SCO) signal and Frequency Modulate Oscillator/ Frequency Modulate Synthesizer (FMO/ FMS) the signal f_{fm}, after the mixing is double side band of transmitter modulation signal $f_c +/- f_{fm}$.

B. Triangle Wave Signal Generator/Intermediate Frequency(IF) Amplifier

1. Triangle Wave Signal Generator: It mainly generate triangular wave signal Vt to modulate FMO, let FMO output a frequency modulation signal.
2. Intermediate Frequency (IF) Amplifier: It is mainly the beat frequency signal enlargement. The key technologies is the filter interception correct beat frequency signal, therefore how to reduce the noise of the signal, Harmonic and Spurious that will be effectively raised the accuracy and resolution the important basis.

C. Antenna Module: The Antenna will mainly be produces RF the frequency modulation to output presents and receive the reflection of instantaneous of echo signal system.

D. Digital Signal Processing (DSP) Module: The DSP module is mainly received the beat frequency signal, after that transforms by Fest Fourier Transform into the frequency signal, and use the related

parameter leads calculated that obtain the range data. As shown Figure 3-5. Microchip dsPIC.

E. Display/Control Module: The module is mainly leads DSP calculated the frequency signal data uses the control program which the personal computing develops to make the demonstration.

The specification table for FMCW radar system is as follows:

RF module electrical characteristecs

- Transmit signal ----------9.42→10.55 GHz
- Sweep Bandwidth----------50MHz→1GHz
- Power----------10mw→100mw
- Antenna beamwidth (Azimuth)------8→12 degree
- Antenna beamwidth (Elevation)-----40→50 degree
- Measure Range ----------5→60 m

3.2 FMCW Radar System Algorithms

A traditional approach for range extraction is use FFT Algorithm, use it to transform time domain to frequency domain with beat frequency signal from RF module. However, following statement and equation is decimation-in-time FFT algorithm. And adding window can focus energy of the spectrum.

3.2.1 Decimation-In-Time FFT Algorithm

In computing the DFT [6], dramatic efficiency results from decomposing the computation into successively smaller DFT computations. In this process,

we exploit both the symmetry and the periodicity of the complex exponential $W_N^{kn} = e^{-j(2\pi/N)kn}$. Algorithms in which the decomposition is based on decomposing the sequence $x[n]$ into successively smaller subsequences are called decimation-in-time algorithms.

The principle of the decimation-in-time algorithm is most conveniently illustrated by considering the special case of N an integer power of 2, i.e., $N = 2^v$. Since N is an even integer, we can consider computing $X[k]$ into two $(N/2)-point$ sequences consisting of the even-numbered points in $x[n]$ and the odd-numbered points in $x[n]$. With $X[k]$ given by

$$X[k] = \sum_{n=0}^{N-1} x[n] W_N^{nk}, \qquad k = 0,1,...,N-1 \tag{3.2.1}$$

And separating $x[n]$ into its even- and odd-numbered points, we obtain

$$X[k] = \sum_{n\ even} x[n] W_N^{nk} + \sum_{n\ \text{odd}} x[n] W_N^{nk} \tag{3.2.2}$$

Or, with the substitution of variables n=2r for n even and n=2r+1 for n odd,

$$X[k] = \sum_{r=0}^{(N/2)-1} x[2r] W_N^{2rk} + \sum_{r=0}^{(N/2)-1} x[2r+1] W_N^{(2r+1)k}$$

$$= \sum_{r=0}^{(N/2)-1} x[2r] \left(W_N^2\right)^{rk} + \sum_{r=0}^{(N/2)-1} x[2r+1] \left(W_N^2\right)^{rk} \tag{3.2.3}$$

But $W_N^2 = W_{N/2}$, since

$$X[k] = \sum_{r=0}^{(N/2)-1} x[2r] W_{N/2}^{rk} + W_N^k \sum_{r=0}^{(N/2)-1} x[2r+1] W_{N/2}^{rk} \tag{3.2.4}$$

$$= G[k] + W_N^k H[k], k = 0,1,...,N-1$$

Each of the sums in Eq (3.2.4) is recognized as an $(N/2)$-point DFT, the first sum being the $(N/2)$-point DFT of the even-numbered points of original sequence and the second being the $(N/2)$-point DFT of the odd-numbered points of the original sequence. Although the index k ranges over N values, $k = 0,1,...,N-1$, each of the sums must be computed only for k between 0 and $(N/2)-1$, since $G[k]$ and $H[k]$ are each periodic in k with period $(N/2)$.After the two DFTs are computed, they are combined according to Eq.(3.2.4) to yield the N-point DFT $X[k]$.Figure 3-6 depicts this computation for $N=8$.In this figure, we have used the signal flow graph representing difference equations. That is, branches entering a node are summed to produce the node variable. When no coefficient is indicated, the branch transmittance is assumed to be unity. For other branches, the transmittance of a branch is an integer power of W_N.

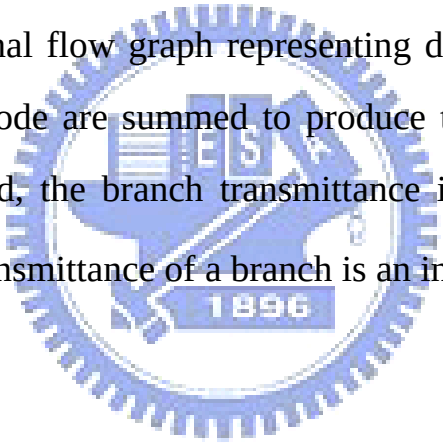

3.2.2 Windows

Spectral leakage is a result of processing finite-duration records when signals being analyzed are not periodic with the observation period. Figure 3-8 [7] shows a periodic extension of a sinusoid that is not periodic in the observation internal. When this signal is processed by a Fourier transform, the discontinuous at the extremities of the observation interval coarse spurious spectral responses known as leakage. Because the FFT essentially considers sequences to be periodic, the condition depicted always prevails except in pathological cases when the signal is periodic in the observation internal. To

reduce the effects of spectral leakage, weighting functions are applied to data. The multiplicative weighting functions, known as windows, are tapered smoothly to zero at the extremities so that the continuity of the periodic extension is enhanced.

The design of tapered windows involves a trade-off between the suppression of leakage sidelobes and reduced spectral resolution. Some commonly used windows are shown in Figure 3-9. These windows are defined by the following equations:

Rectangular

$$w[n] = \begin{cases} 1, & 0 \le n \le M \\ 0, & otherwise \end{cases} \tag{3.2.5}$$

Hanning

$$w[n] = \begin{cases} 0.5 - 0.5\cos(2\pi n / M), & 0 \le n \le M \\ 0, & otherwise \end{cases} \tag{3.2.6}$$

Hamming

$$w[n] = \begin{cases} 0.54 - 0.46\cos(2\pi n / M), & 0 \le n \le M \\ 0, & otherwise \end{cases} \tag{3.2.7}$$

3.3 Range Resolution

Range resolution [8], denoted as ΔR, is radar metric that describes its ability to detect targets in close proximity to each other as distinct objects. Radar systems are normally designed to operate between a minimum range R_{min}, and maximum range R_{max}. The distance between R_{min} and R_{max} is divided into M range bins (gates), each of width ΔR,

$$M = \left(R_{\max} - R_{\min} \right) / \Delta R \tag{3.3.1}$$

Targets separated by at least ΔR will be completely resolved in range. Targets within the same range bin can be resolved in cross range (azimuth) utilizing signal processing techniques. Consider two targets located at ranges R_1 and R_2, corresponding to time delays t_1 and t_2, respectively. Denote the difference between those two ranges as ΔR:

$$\Delta R = R_2 - R_1 = c\frac{\left(t_2 - t_1 \right)}{2} = c\frac{\delta t}{2} \tag{3.3.2}$$

First, assume that the two targets are separated by $\tau c/4$, where τ is the pulse width. In this case, when the pulse trailing edge strikes target 2 the leading edge would have traveled backwards a distance τc, and the returned pulse would be composed of returns from both targets, as shown in figure 3-10(a). However, if the two targets are at least $\tau c/2$ apart, then as the pulse trailing edge strikes the first target the leading edge sill start to return from target 2, and two distinct returned pulses will be produced, as illustrated by figure 3-10(b). Thus, ΔR should be greater or equal to $\tau c/2$. And since the radar bandwidth B is equal to $1/\tau$, then

$$\Delta R = \frac{c\tau}{2} = \frac{c}{2B} \tag{3.3.3}$$

In general, radar users and designers alike seek to minimize ΔR in order to enhance the radar performance. As suggested by equation (3.3.3), in order to achieve fine range resolution one must minimize the pulse width. However, this will reduce the average transmitted power and increase the operating bandwidth. Achieving fine range resolution while maintaining adequate average transmitted power can be accomplished by using pulse compression techniques. So this

problem will be researched to solution.

Chapter 4

Increase Accuracy of Measuring Frequency

In the measuring range use FM-CW liquid level radar system, the accuracy has strict requested quite. A traditional approach for range extraction does use FFT to transform time domain into frequency domain from beat frequency signal. When use FFT to analysis the signal spectrum, the frequency accuracy is mainly affected by aliasing, quantization error, leakage, picket fence effects. Both the aliasing and quantization produce from analog to digital converter procedure, the leakage and picket fence effects produce from FFT procedure. So we research how to eliminate these questions, and we will propose a novel method to eliminate effect from picket fence effects.

4.1 Increase Accuracy Algorithm

Literature review, these propose algorithms to increase frequency accuracy of the spectrum. For example: Chirp-Z Transform Algorithm (CZT), Cubic Spline Interpolation, Fast Frequency Estimation Algorithm (FFEA) and Energy Centrobaric Method etc.

4.1.1 Cubic Spline Algorithm

A mechanical means of producing smooth interpolating curves, heavily used in the past in the shipbuilding and aircraft industies, consists in the use of a thin, flexible batten or spline, held on place by weghts. This spline bends in such a way, that its internal energy due to bending is minimal, consistent with the interpolation constraints imposed on it. At any point of the spline, the bending energy depends on the curvature there. The fitting of a polynomial curve to a set of data points has applications in CAD (computer-assisted design), CAM (computer-assisted manufacturing), and computer graphics systems. An operator wants to draw a smooth curve through data points that are not subject to error. Traditionally, it was common to use a french curve or an architect's spline and subjectively draw a curve the looks smooth when viewed by the eye. Mathematically, it is possible to construct cubic functions $S_k(x)$ on each interval $[x_k, x_{k+1}]$ so that the resulting piecewise curve $y = S(x)$ and its first and second derivatives are all continuous on the larger interval $[x_0, x_N]$. The continuity of $S'(x)$ means that the graph $y = S(x)$ will not have sharp corners. The continuity of $S''(x)$ means that the radius of curvature is defined at each point. [9]

Suppose that $\{(x_k, y_k)\}_{k=0}^{N}$ are $N + 1$ points, where $a = x_0 < x_1 < \cdots < x_N = b$. The function $S(x)$ is called a cubic spline if there exist N cubic polynomials $S_k(x)$ with coefficients $S_{k,}0, S_{k,}1, S_{k,}2$, and $S_{k,}3$ that satisfy the following properties:

I. $S(x) = S_k(x) = s_{k,0} + s_{k,1}(x - x_k) + s_{k,2}(x - x_k)^2 + s_{k,3}(x - x_k)^3$

$for\ \mathrm{x} \in [\mathrm{x}_k, x_{k+1}]\ and\ k = 0,1,...,N-1.$

II. $S(x_k) = y_k$ for k=0,1,...,N.

III. $S_k(x_{k+1}) = S_{k+1}(\mathrm{x}_{k+1})$ for k=0,1,...,N-2.

IV. $S_k'(x_{k+1}) = S_{k+1}'(x_{k+1})$ for k=0,1,...,N-2.

V. $S_k''(x_{k+1}) = S_{k+1}''(x_{k+1})$ for k=0,1,...,N-2.

Property I states that $S(x)$ consists of piecewise cubics. Property II states that the piecewise cubics interploate the given set of data points. Properties III and IV require that the piecewise cubics represent a smooth continuous function. Property V states that the second derivative of the resulting function is also continuous.

Let us tr to determine if it is possible to construct a cubic spline that satisfies properties I through V. Each cubic polynomial $S_k(x)$ has four unknown constants $(S_{k,0}, S_{k,1}, S_{k,2}, \text{ and } S_{k,3})$; hence here are $4N$ degrees of freedom or conditions that must be specified. The data points supply $N+1$ conditions, and properties III, IV ,and V each supply $N-1$ conditions. Hence, $N+1+3(N-1) = 4N-2$ conditions are specified. This leaves us two additional degrees of freedom. We will call them endpoint constraints: they will involve either $S'(x)$ or $S''(x)$ at x_0 and x_N and will be discussed later. We now proceed with the construction.

Since $S(x)$ is piecewise cubic, its second derivative $S''(x)$ is piecewise linear on $[x_0, x_N]$. The linear Lagrange interploation foumula gives the following representation for $S''(x) = S_k''(x)$:

$$S_k^{"}(k) = S^{"}(s_k)\frac{x - x_{k+1}}{x_k - x_{k+1}} + S^{"}(x_{k+1})\frac{x - x_k}{x_{k+1} - x_k} \qquad (4.1.1)$$

Use $m_k = S''(x_k)$, $m_{k+1} = S''(x_{k+1})$, and $h_k = x_{k+1} - x_k$ in (4.1.1)to get

$$S_k^{"}(k) = \frac{m_k}{k_k}(x_{k+1} - x) + \frac{m_{k+1}}{h_k}(x - x_k) \qquad (4.1.2)$$

For $x_k \le x \le x_{k+1}$ and $k = 0,1,\ldots,N-1$. Integrating (4.1.2) twice will introduce two constants of integration, and the result can be manipulated so that it has the form

$$S_k(x) = \frac{m_k}{6h_k}(x_{k+1} - x)^3 + \frac{m_{k+1}}{6h_k}(x - x_k)^3 + p_k(x_{k+1} - x) + q_k(x - x_k) \qquad (4.1.3)$$

Substitution x_k and x_{k+1} into equation (4.1.3) and using the values $y_k = S_k(x_k)$ and $y_{k+1} = S_k(x_{k+1})$ yields the following equations that involve p_k and q_k, respectively:

$$y_k = \frac{m_k}{6}h_k^2 + p_k h_k \text{ and } y_{k+1} = \frac{m_{k+1}}{6}h_k^2 + p_k h_k \qquad (4.1.4)$$

These two equations are easily solved for p_k and q_k, and when these values are substituted into equation (4.1.4), the result is the following expression for the cubic function $S_k(x)$:

$$S_k(x) = -\frac{m_k}{6h_k}(x_{k+1} - x)^3 + \frac{m_{k+1}}{6h_k}(x_{k+1} - x)^3 + \left(\frac{y_k}{h_k} - \frac{m_k h_k}{6}\right)(x_{k+1} - x) + \left(\frac{y_{k+1}}{h_k} - \frac{m_{k+1}h_k}{6}\right)(x - x_k) \qquad (4.1.5)$$

Notice that the representation (4.1.5) has been reduced to a form that involves

only the unknown coefficients $\{m_k\}$. To find these values, we must use the derivative of (4.1.5), which is

$$S_k^{'}(x) = -\frac{m_k}{2h_k}(x_{k+1} - x)^2 + \frac{m_{k+1}}{2h_k}(x - x_k)^2 - \left(\frac{y_k}{h_k} - \frac{m_k h_k}{6}\right) + \frac{y_{k+1}}{h_k} - \frac{m_{k+1}h_k}{h_k} \tag{4.1.6}$$

Evaluating (4.1.6) at x_k and simplifying the result yield

$$S_k^{'}(x_k) = -\frac{m_k}{3}h_k - \frac{m_{k+1}}{6}h_k + d_k \tag{4.1.7}$$

$$where\ d_k = \frac{y_{k+1} - y_k}{h_k}$$

Similarly, we can replace k by $k-1$ in (4.1.7) to get the expression for $S_{k-1}^{'}(x)$ and evaluate to at x_k to obtain

$$S_{k-1}^{'}(x_k) = \frac{m_k}{3}h_{k-1} + \frac{m_{k-1}}{6}h_{k-1} + d_{k-1} \tag{4.1.8}$$

Now use property IV and equation (4.1.7) and (4.1.8) to obtain an improtant relation involving m_{k-1}, m_k, and m_{k+1}:

$$h_{k-1}m_{k-1} + 2(h_{k-1} + h_k)m_k + h_k m_{k+1} = u_k \tag{4.1.9}$$

Where $u_k = 6(d_k - d_{k-1})$ for $k = 1,2,\ldots,N-1$. So according to above equation, use the MATLAB software to simulate a sinusoid wave and compare linear interpolation with cubic spline interpolation, respectively. Show the figure 4-1.

4.1.2 Chirp-Z Transform Algorithm

Another algorithm based on expressing the DFT as a convolution is referred to as the chirp transform algorithm (CTA) [6]. This algorithm is not optimal in minimizing any measure of computational complexity, but it has been useful in a variety of applications, particularly when implemented in technologies that are well suited to doing convolution with a fixed, prespecified impulse response. The CTA is also more flexible than the FFT, since it can be used to compute any set of equally spaced samples of the Fourier transform on the unit circle.

To derive the CTA, we let $x[n]$ denote an N-point sequence and $X\left(e^{jw}\right)$ its Fourier transform. We consider the evaluation of M samples of $X\left(e^{jw}\right)$ that are equally spaced in angle on the unit circle, as indicated in Figure 3-7, i.e., at frequencies

$$\omega_k = \omega_0 + k\Delta\omega, k = 0,1,...,M-1 \tag{4.1.10}$$

Where ω_0 is the starting frequency.

$\Delta\omega$ is the frequency increment.

The starting frequency ω_0 and the frequency increment $\Delta\omega$ can be chosen arbitrarily. The Fourier transform corresponding to this more general set of frequency samples is given by

$$X\left(e^{j\omega_k}\right) = \sum_{n=0}^{N-1} x[n]e^{-j\omega_k n} \tag{4.1.11}$$

Or, with W defined as

$$W = e^{-j\Delta\omega} \tag{4.1.12}$$

And using Eq. (4.1.10)

$$X\left(e^{j\omega_k}\right)=\sum_{n=0}^{N-1}x[n]e^{-j\omega_0 n}W^{nk} \tag{4.1.13}$$

To express $X\left(e^{j\omega_k}\right)$ as a convolution, we use the identity

$$nk=\frac{1}{2}\left[n^2+k^2-(k-n)^2\right] \tag{4.1.14}$$

To express Eq.(4.1.13)

$$X\left(e^{j\omega_k}\right)=\sum_{n=0}^{N-1}x[n]e^{-j\omega_0 n}W^{\frac{n^2}{2}}W^{\frac{k^2}{2}}W^{\frac{-(k-n)^2}{2}} \tag{4.1.15}$$

Letting

$$g[n]=x[n]e^{-j\omega_0 n}W^{\frac{n^2}{2}} \tag{4.1.16}$$

We can then write

$$X\left(e^{j\omega_k}\right)=W^{\frac{k^2}{2}}\left(\sum_{n=0}^{N-1}g[n]W^{\frac{-(k-n)^2}{2}}\right) \tag{4.1.17}$$

In preparation for interpreting Eq.(4.1.17) as the output of a linear time-invariant system, we obtain more familiar notation by replacing k by n and n by k in Eq.(4.1.17)

$$X\left(e^{j\omega_n}\right)=W^{\frac{n^2}{2}}\left(\sum_{k=0}^{N-1}g[k]W^{\frac{-(n-k)^2}{2}}\right) \tag{4.1.18}$$

In the form of Eq.(4.1.18), $X\left(e^{j\omega_n}\right)$ corresponds to the convolution of the sequence $g[n]$ with the sequence $W^{-\frac{n^2}{2}}$, followed by multiplication by the sequence $W^{\frac{n^2}{2}}$. The output sequence, indexed on the independent variable n, is the sequence of frequency samples $X\left(e^{j\omega_n}\right)$ .With this interpretation, the

computation of Eq. (4.1.18) is as depicted in Figure 3-8. The sequence $W^{-\frac{n^2}{2}}$ can be thought of as a complex exponential sequence with linearly increasing frequency $n\Delta w$. In radar systems, such signals are called chirp signals-hence the name chirp transform.

According to above statement, and use the Matlab software to simulate. Show the Figure 4-3. Chirp-Z Transform Algorithm can see distinct the peak frequency from FFT, It can raise accuracy.

Therefore, we compare the measuring results of two methods with FFT. Use the MATLAB software to simulate that input frequency 60 Hz to 100 Hz of the sinusoid. Moreover use Cubic Splne, Chirp-Z transform and fast Fourier transform method to measure frequency, and compare the error with input frequency. Show the figure 4-4. We can get error within or no more than 0.5 Hz by Chirp-Z transform, but Chirp-Z transform algorithm has a defect, because that can only see a small frequency band.

4.1.3 Energy Centrobaric Method

The energy centrobaric algorithm is a suitable method from the literature review. In the very clear environment, the accuracy can achieve 1% of the frequency error [10] [11]. Energy centrobaric Algorithm uses the window function to focus power of the signal, and we would calibrate using this method by energy centrobaric algorithm.

Take Hanning window for example; research the window function property of the spectral analysis. Hanning window define:

$$W(n)=0.5-0.5\cos(2\pi n/N)$$
$$n=0,1,2,\ldots,N-1 \tag{4.2.1}$$

Its spectrum function is

$$y(x)=\frac{\sin\pi x}{\pi x}\cdot\frac{1}{2(1-x^2)} \tag{4.2.2}$$

Let power spectrum is $(x)=y^2(x)$，we can get

$$G(x)=\frac{\sin^2\pi x}{4\pi^2x^2(1-x^2)^2} \tag{4.2.3}$$

To any a definite x, when $n\to\infty$，G(x) satisfies the below equation

$$\sum_{i=-n}^{n}G(x+i)\cdot(x+i)=0 \tag{4.2.4}$$

proof:

$$\sum_{i=-n}^{n}G(x+i)\cdot(x+i)=$$
$$\sum_{i=-n}^{n}\frac{\sin^2[\pi(x+i)]}{4\pi^2(x+i)^2[1-(x+i)^2]^2}\cdot(x-i)$$
$$=\sum_{i=-n}^{n}\frac{\sin^2(\pi x)}{16\pi^2}[\frac{1}{(x+i-1)^2}-\frac{1}{(x-i+1)^2}+$$
$$\frac{4}{x-i}-\frac{2}{x+i-1}-\frac{2}{x+i+1}] \tag{4.2.5}$$
$$=\frac{-\sin^2(\pi x)}{16\pi^2(n-x)^2(n+x+1)^2}+$$
$$\frac{\sin^2(\pi x)}{16\pi^2(n-x)^2(n-x-1)^2}$$

Obviously, when $n\to\infty$, equation (4.2.4) establishment.

According to equation (4.2.4) indication, the Hanning window separate frequency spectrum's energy center of gravity approaches the origin of coordinates infinitely. Due to the sidelobe of the power spectrum of the Hanning window is very small. According to energy center of gravity property, if $x \in [-0.5,0.5]$, it can use the big several spectral line of mainlobe within power spectrum to measure precisely the central coordinate of mainloab.

Assume mainlobe of the frequency spectrum is

$$Y(x) = A\frac{\sin^2\left[\pi(x-x_0)\right]}{4\pi^2(x-x_0)^2\left[1-(x-x_0)^2\right]^2} \tag{4.2.6}$$

Equal equation (4.2.3) multiply coefficient A and shift to $x = x_0$, x_0 and A are frequency and amplitude of the analysis signal respectively, Y_n is maximum value of the spectral line in the mainlobe. Show the figure 4-4. When $n \to \infty$, according to Hanning window energy center of gravity property has

$$\sum_{i=-n}^{n} Y_i \cdot (x - x_0 + i) = 0 \tag{4.2.7}$$

Simplification above equation

$$\sum_{i=-n}^{n} Y_i \cdot (x+i) - \sum_{i=-n}^{n} Y_i \cdot x_0 = 0 \tag{4.2.8}$$

Accroding to equation (4.2.8) can get the center of manlobe

$$x_0 = \frac{\sum_{i=-n}^{n} Y_i \cdot (x+i)}{\sum_{i=-n}^{n} Y_i} \tag{4.2.9}$$

So, follow above these equations. We can get the final equations. Use the two spectral lines within mainlobe of the amplitude spectrum Y_k, Y_{k+1}, it

solve the energy center of gravity x_0 after shift.

$$x_0 = \frac{(K-1)Y_K + (K+2)Y_{K+1}}{Y_K + Y_{K+1}} = K + \frac{2Y_{K+1} - Y_K}{Y_K + Y_{K+1}} \tag{4.2.10}$$

Likewise, use Y_{k-1}, Y_k spectral lines solve energy center of gravity is

$$x_0 = K + \frac{Y_K - 2Y_{K-1}}{Y_K + Y_{K+1}} \tag{4.2.11}$$

Let $x_0 = K + \Delta K$, we can get frequency calibration equation

$$\Delta K = \begin{cases} \frac{2Y_{K+1} - Y_K}{Y_K + Y_{K+1}} & (Y_{K+1} \geq Y_{K-1}) \\ \frac{Y_K - 2Y_{K-1}}{Y_K + Y_{K+1}} & (Y_{K+1} < Y_{K-1}) \end{cases} \tag{4.2.12}$$

Finally, above equation is frequency calibration equation. Then we compare this energy centrobaric method with gradient search method which we propose a novel ideal.

4.2 A Proposed Method - Gradient Search Method

A novel method for the FMCW radar measuring system will be proposed. The conventional fast Fourier transform (FFT) method is timesaving, but the accuracy of the frequency estimation from discrete spectra is limited due to its leakage and picket fence effects. In order to improve the measurement accuracy, some rectification methods for discrete spectra based on FFT, such as cubic spline interpolated FFT and energy centrobaric methods, have been proposed. But accuracy cannot reach under 1% of the error. Therefore, we propose a novel method to solve this question.

Its detailed process that receive the beat frequency (f_b) signal from RF module, and perform fast Fourier transform after adding hanning window

function. Transfer the time domain signal to frequency domain signal, and search amplitude spectrum. Find the coarse peak frequency (F_{mid}) from the fast Fourier transform measuring, and use we proposed gradient search method to do detail calibration. Show the figure 4-5.

Following below the deriving equation, is the gradient search method idea and procedure.

In the time domain, fast Fourier transform define

$$x(t) = \sum_{n=-\infty}^{\infty} x_n e^{j2\pi \frac{n}{T_0} t} \tag{4.3.1}$$

Differential the time

$$\frac{dx(t)}{dt} = \frac{d\sum_{n=-\infty}^{\infty} x_n e^{j2\pi \frac{n}{T_0} t}}{dt} \tag{4.3.2}$$

We can get the below function

$$x'(t) = j2\pi \frac{n}{T_0} \sum_{n=-\infty}^{n} x_n e^{j2\pi \frac{n}{T_0} t} \tag{4.3.3}$$

This result can do to search slope function, just need lead the peak frequency value, it will get the peal value slope.

From the frequency domain point derive

$$X(\omega) = M(\omega) \cdot e^{j\phi(\omega)} \tag{4.3.4}$$

Differential to the frequency

$$X'(\omega) = M'(\omega) \cdot e^{j\phi(\omega)} + jM(\omega) \cdot \phi'(\omega) \cdot e^{j\phi(\omega)}$$

$$\frac{X'(\omega)}{X(\omega)} = \frac{M'(\omega)}{M(\omega)} + j\phi'(\omega) \tag{4.3.5}$$

We can divide into real part and imaginary part

Real part: (Magnitude difference ratio)

$$\mathrm{Re}\left\{\frac{X^{'}(\omega)}{X(\omega)}\right\}=\frac{M^{'}(\omega)}{M(\omega)} \tag{4.3.6}$$

Imaginary part: (Phase gradient)

$$\mathrm{Im}\left\{\frac{X^{'}(\omega)}{X(\omega)}\right\}=\phi^{'}(\omega) \tag{4.3.7}$$

The magnitude of digital Fourier transform is

$$\left|X(\omega)\right|=M(\omega) \tag{4.3.8}$$

So its slope could be represented as

$$\left|X(\omega)\right|^{'}=M^{'}(\omega) \tag{4.3.9}$$

Assume that $X(\omega) = A_r + jA_i$, and $X'(\omega) = B_r + jB_i$, then divide by

$$M^{'}(\omega)=\mathrm{Re}\left\{\frac{X^{'}(\omega)}{X(\omega)}\cdot M(\omega)\right\} \tag{4.3.10}$$

The sign of $M'(\omega)$ is

$$\mathrm{Re}\left\{\frac{X^{'}(\omega)}{X(\omega)}\cdot M(\omega)\right\}=\mathrm{Re}\left\{\left(B_r+jB_i\right)\left(A_r-jA_i\right)\right\} \tag{4.3.11}$$

$$=A_rB_r+A_iB_i$$

The result is real part multiply differential real part plus imaginary part multiply differential imaginary part. Use this method to decide that slope is positive or negative. If the slope sign is negative, it represents the actual frequency which locates at measuring frequency left side. Show the figure 4-6.

Therefore we replace $F_{mid} = F_{hi}$, otherwise $F_{min} = F_{lo}$, then make $F_{mid} = (F_{hi} + F_{lo})$. Follow this method repeatedly several times, about ten times. It would get the better of accuracy frequency (F_{fine}). Finally, use the F_{fine}

frequency to measure range $R = F_{fine} \cdot c/2k$ (R represent range, c represent light velocity, k represent transmit signal slope parameter), that accuracy would reach within error 1%.

Finally we use MATLAB software simulation to compare gradient search method with energy centrobaric method results.

Chapter 5
Simulate and Realization with MCU

In the FMCW radar measuring system has many un-know noise existence. Therefore we simulate some conditions which could happen. For example, false target near real target bring to frequency shift, etc…. and we simulate the power of noise existence, then gradient search method can be excellent. So we simulate these questions to compare gradient search method with energy centrobaric method, these results will show in this chapter.

5.1 Simulate with MATLAB Software

Use the above methods to simulate experiment, and compare gradient search method with energy centrobaric method. The simulation parameters are sampling frequency 14 kHz, fast Fourier transform length 512 points, input sinusoidal signal, input frequency 500 Hz to 7000 Hz, and simulate without noise environment. The Energy centrobaric method can calibrate frequency within 0.06 Hz of the error frequency, however gradient search method can calibrate within 0.01 Hz of the error frequency. Show the figure 5-1. Continuous, add white noise into simulation, and we compare two methods to resist noise ability. Show the figure 5-2. Follow the results; energy centrobaric method calibration was effected with white noise bigger than gradient search method. So we can know the gradient search method better then energy centrobaric method.

5.2 Simulate False Target near Real Target with MATLAB Software

In the FMCW radar measuring system, when we detect a target range, if it has a false target near the real target which we want detect, cause the frequency shift error. So we make a small power target signal near peak frequency 30 Hz, the result is gradient search method better than energy centrobaric method. Show the figure 5-3.

Because of the small power target signal will affect the power spectrum amplitude, causing the peak amplitude shift right or left side. So frequency will be shifted.

5.3 Realization with MCU

We use dsPIC-16 bits micro controller unit (MCU) from Microchip company produce to realize gradient search method and energy centrobaric method. This MCU includes 12 bits of analog to digital converter and maximum sampling frequency 500 kHz. Therefore we use sampling frequency 14 kHz and fast Fourier transforms length 512 points. It will have fast Fourier transform bins 27 Hz, and makes interval positive and negative 250 mm error.

The experiment procedure is using function generator to produce sinusoidal signal, then measure frequency from 500 Hz to 7 kHz by micro controller unit. And the digital processing procedure is

1. Initialization.
2. Analog to digital convertor 512 points.

3. Add Hanning window.
4. Fast Fourier transforms 512 points.
5. Search spectrum to find coarse peak frequency.
6. Calculate the positive or negative slope.
7. Run 10 times.
8. Find the fine frequency.
9. Transform to range.
10. Show in the LCD.

The flow chart is shown the figure 5-4. The experiment results, energy centrobaric method root mean square error (RMSE) is 0.0343 Hz, and gradient search method root mean square error is 0.0127 Hz. Follow this results, gradient search method can measure accuracy frequency, and it is better than energy centrobaric method. Show the figure 5-5.

Chapter 6

Conclusion

In the FMCW measuring level system, use this gradient search method of this thesis to measure frequency that will obtain high precision frequency. But gradient search method has a defect. Although it can measure high accuracy frequency, that elapses time too much. Therefore, it needs match the hardware specification.

In the thesis, we compare measuring accuracy and elapsing time from gradient search method and energy centrobaric method, and add white noise to compare. The gradient search method results except elapsing time that accuracy and resisting noise ability is better than energy centrobaric method. Actually, that must be having noise and background noise as FMCW radar system detecting. Therefore we cannot trust results from energy centrobaric method measuring in the application.

If we can combine gradient search method and energy centrobaric method, it is a best combination. Preliminary conception is using energy centrobaric method to find the close correct frequency, continuous using gradient search method to search fine frequency. So this combination method can reduce searching times from gradient search method and raise accuracy frequency from energy centrobaric method.

This thesis implements gradient search method and energy centrobaric method with MCU. It obtained results different simulation results from MATLAB software that is “Time”. Because of oscillator is not the same, but

elapsing time of gradient search method is about 0.0002 sec for implemented one times from computer oscillator. If gradient search method implement 10 times, its elapsing time are more than 2.5 times energy centrobaric method.

Reference

[1] David M. Pozar; Microwave Engineering, 3rded. : Wiley ,pp.661

[2] Skolnik, Merrill I.; Introduction to radar systems :McGraw-Hill

[3] 陳瑜正, 6GHz縮小化頻率調變連續波雷達系統(6GHz Compact Size Frequency Modulation Continuous Wave Radar System) 國立交通大學電信工程學系,碩士論文, 2007

[4] Qi Guoqing and Jia Xinle, Improvement of Measurement Accuracy of FMCW Level Radar, Electronic and Information Engineering College and Marine Engineering Institute Dalian Maritime University, Dalian 116026, P.R. China

[5] Samuel O.Piper, FMCW Radar Courses, Senior Research Engineer Sensors and Electromagnetic Applications Laboratory

[6] Alen V.Oppenheim, Ronald W.Schafer and John R.Buck, DISCRETE-TIME SIGNAL PROCESSING,Published by Prentice-Hall, Inc. Upper Saddle River, New Jersey 07458

[7] Dean L.Mensa, High Resolution Radar Cross-Section Imaging, Artech House, Boston.London

[8] Bassem R.Mahafza and Atef Z.Elsherbeni, MATLAB Simulations for Radar Systems Design, CHAPMAN & HALL/CRC A CRC Press Company Boca Raton London New York Washington, D.C.

[9] John H.Mathews and Kurtis K. Fink, Numerical Methods Using Matlab, 4th Edition, 2004, Prentice-Hall Inc. Upper Saddle River, New Jersey, USA

[10]丁康, 江利旗, 離散頻譜的能量重心校正法, 汕頭大學機械電子工程系, 廣州市自動化工程研製中心.

[11]謝明, 丁康, 頻譜分析的校正方法, 重慶大學汽車工程系.

Figures

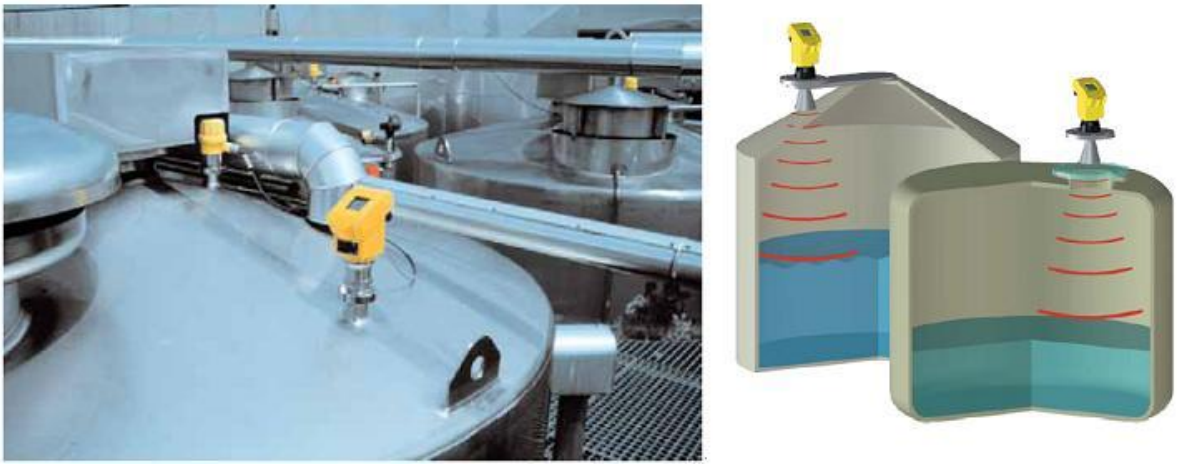

Figure1- 1: FMCW Level Radar System.

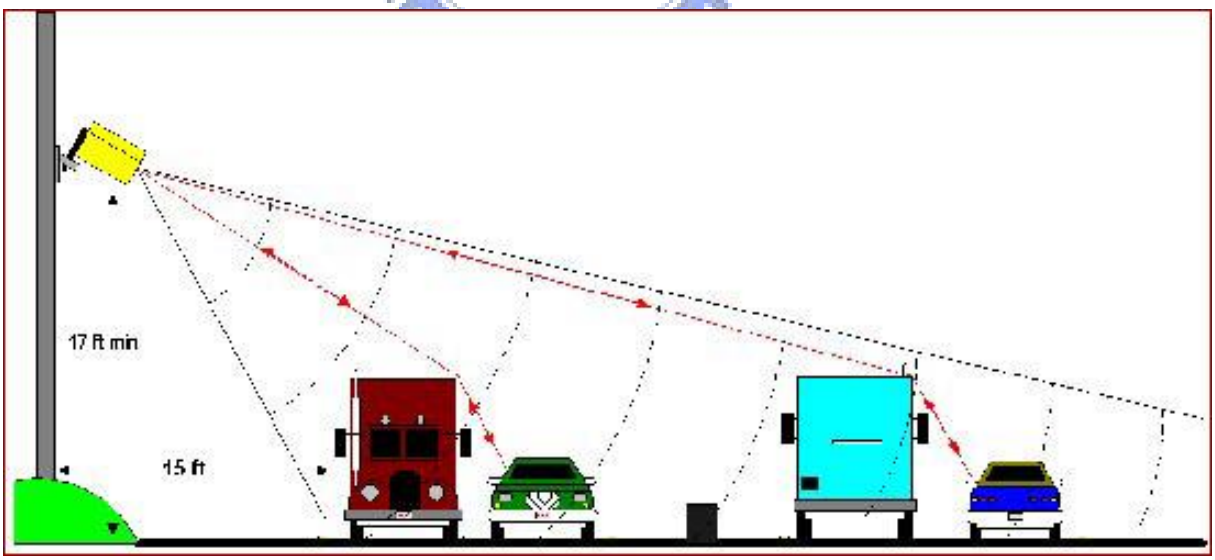

Figure1- 2: Microwave Radar Vehicle Detector.

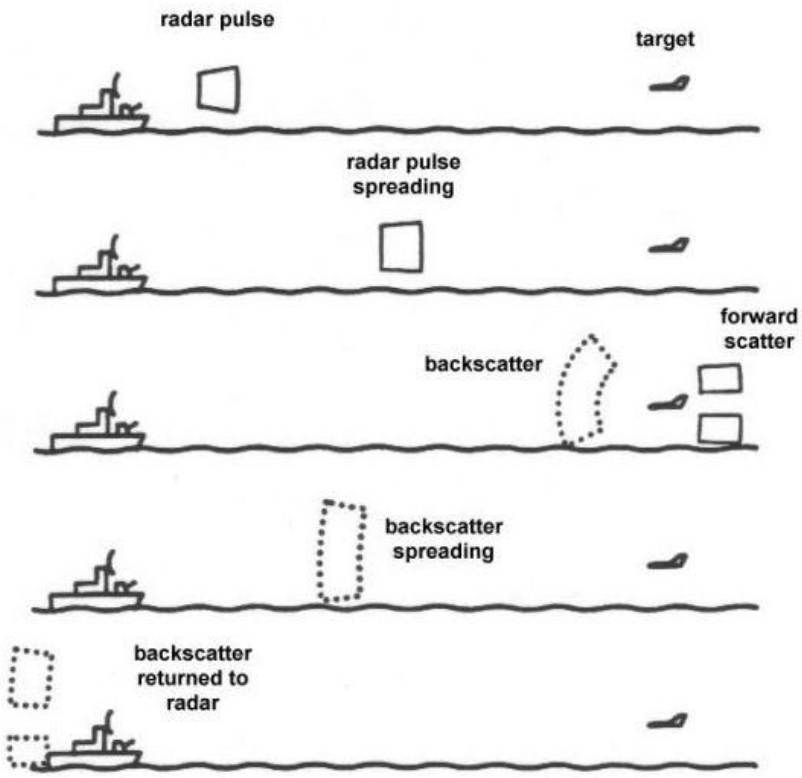

Figure 2- 1: Diagram of Radar System.

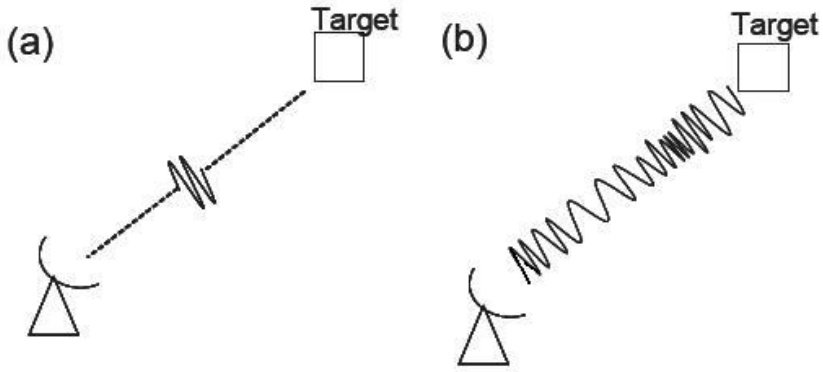

Figure 2- 2: (a) Pulse Radar diagram. (b) FMCW Radar diagram.

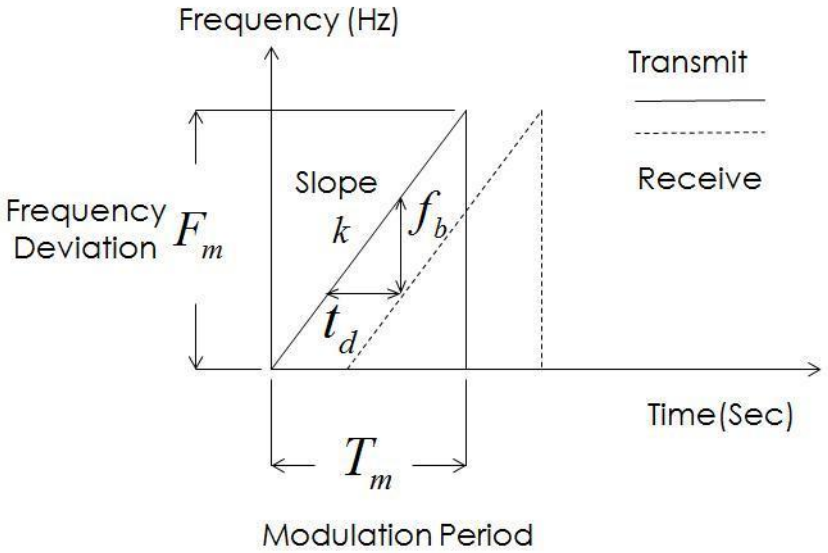

Sawtooth Waveform

Figure 2- 3: Frequency Modulation Wave and Receiving Signal without Relative Velocity.

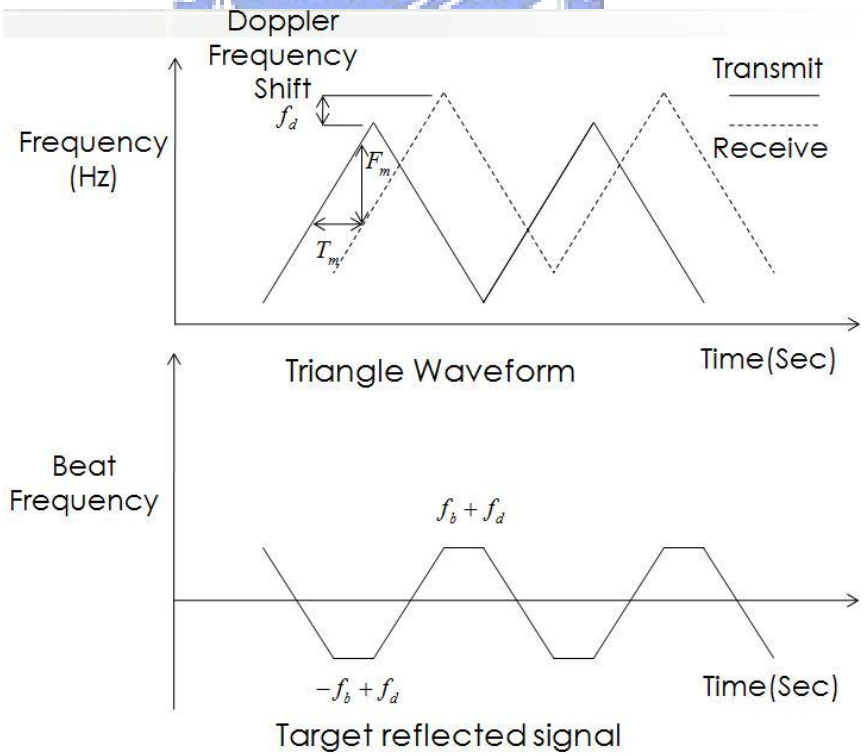

Figure 2- 4: Frequency Modulation Wave and Receiving with Relative Velocity.

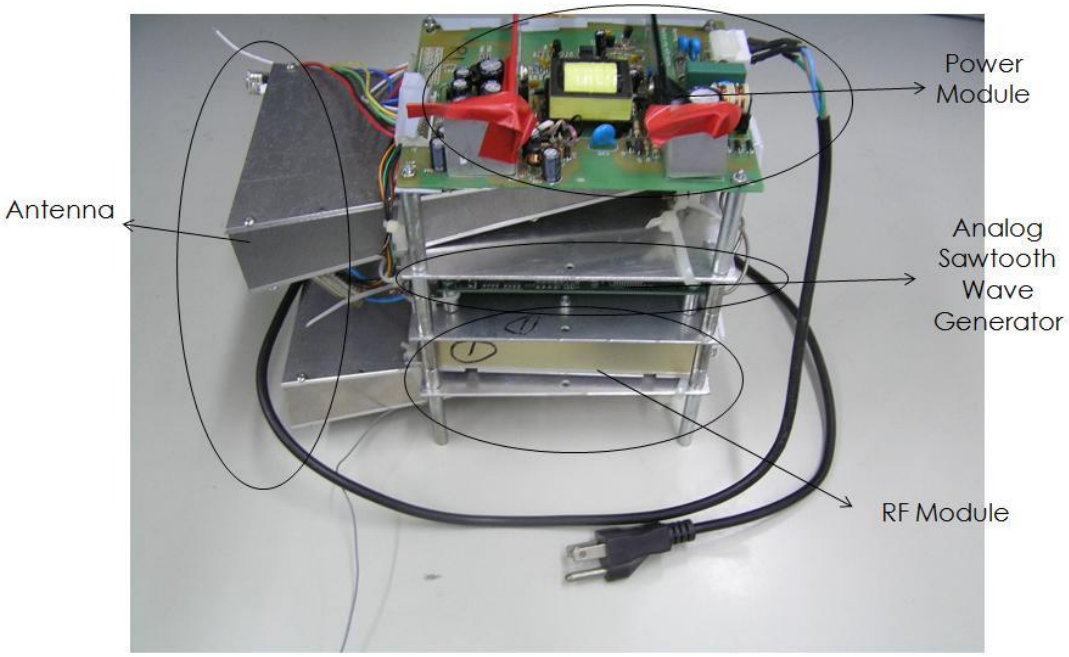

Figure 3- 1: FMCW Radar System.

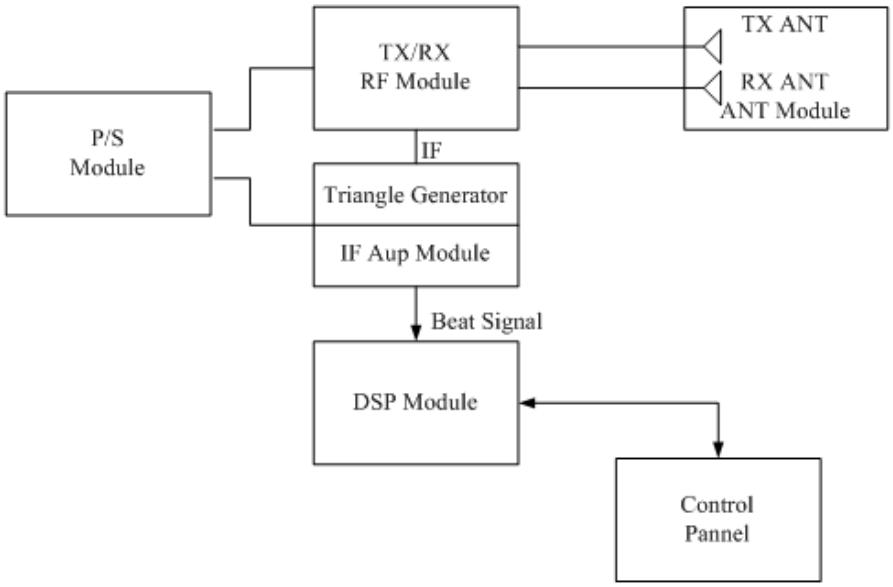

Figure 3- 2: FMCW System Diagram.

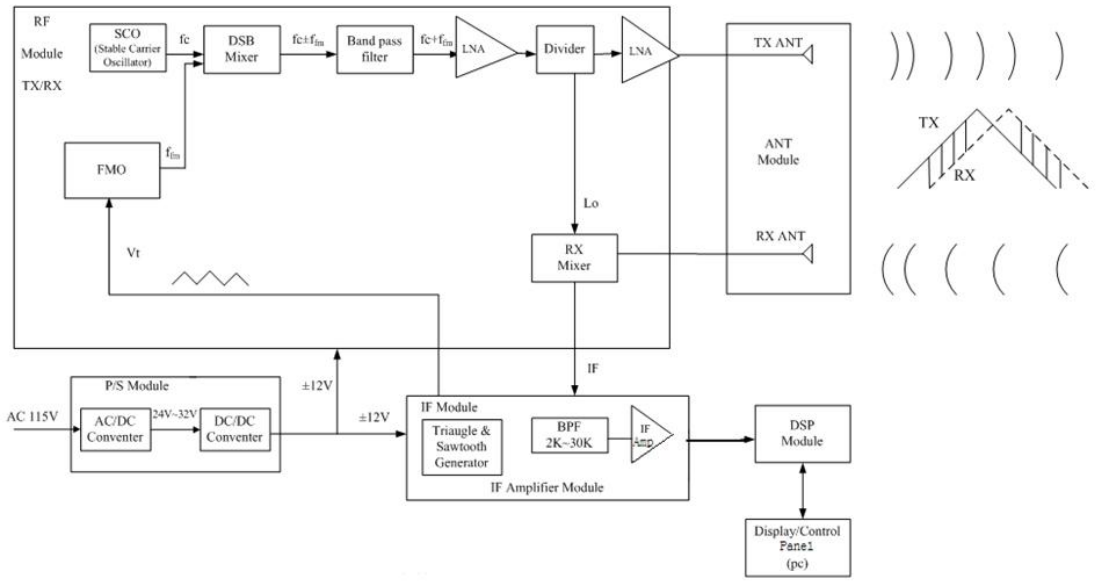

Figure 3- 3: Typical FMCW Radar System Function Diagram.

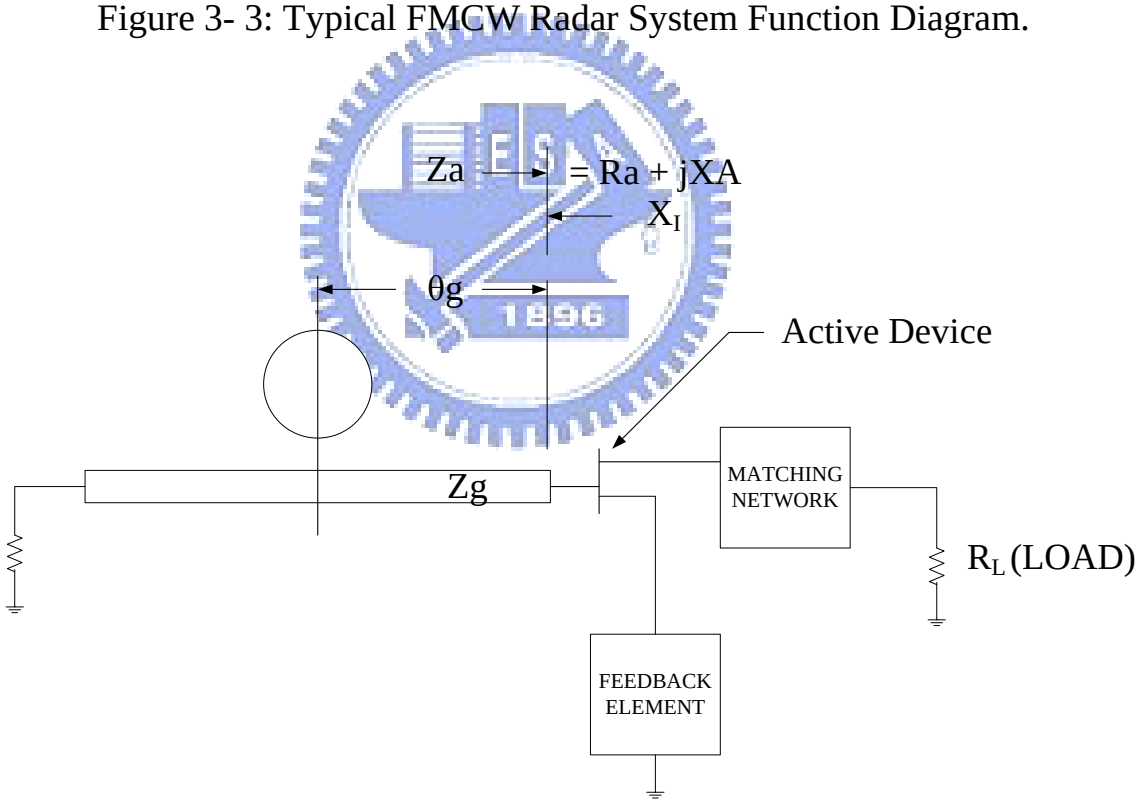

Figure 3- 4: SCO Feedback For Electric Circuit Schematic.

Figure 3- 5: Microchip dsPIC APP021 And ICD2.

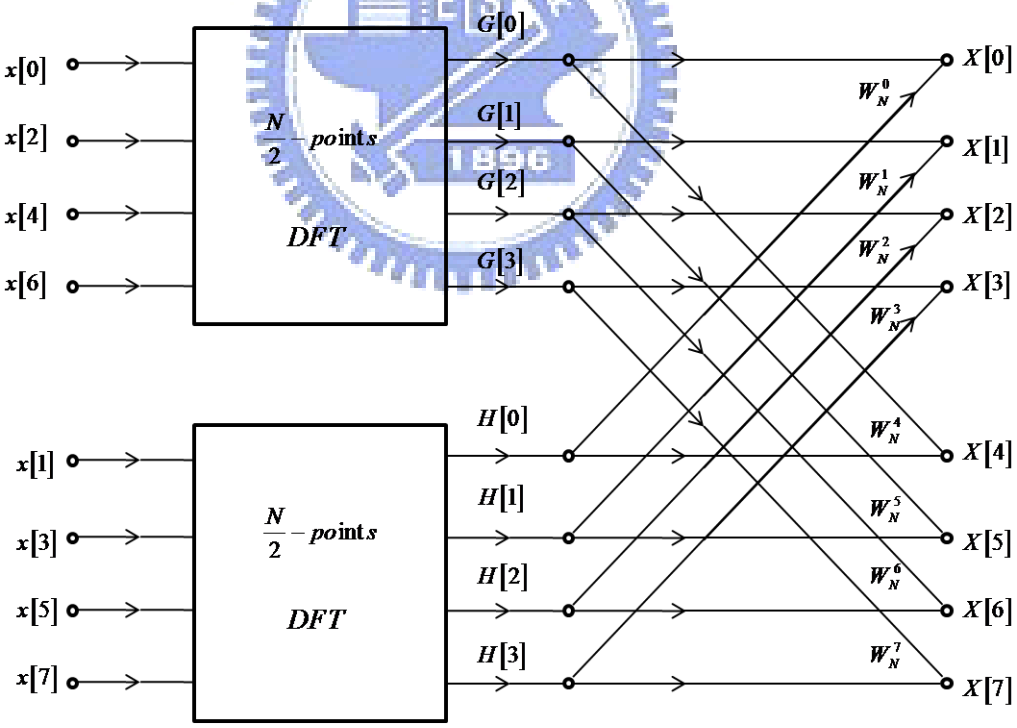

Figure 3- 6: Flow Graph of the Decimation-In-Time Decomposition of an N-point DFT computation into two (N/2)-point DFT computations (N=8).

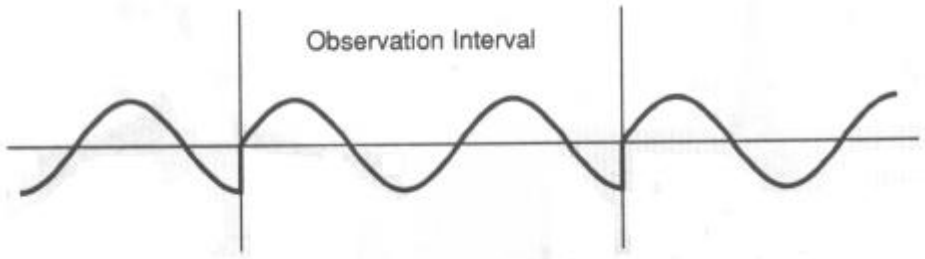

Figure 3- 7: Periodic extension of signal not periodic in observation interval.

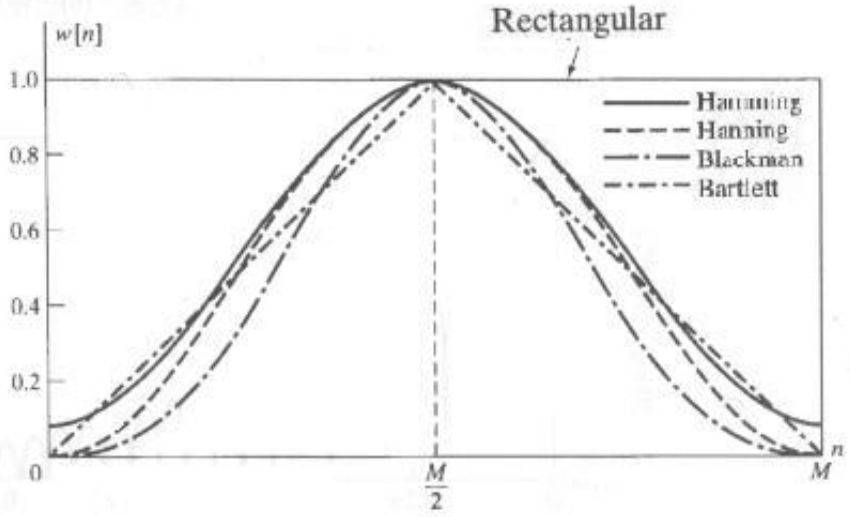

Figure 3- 8: Commonly used windows.

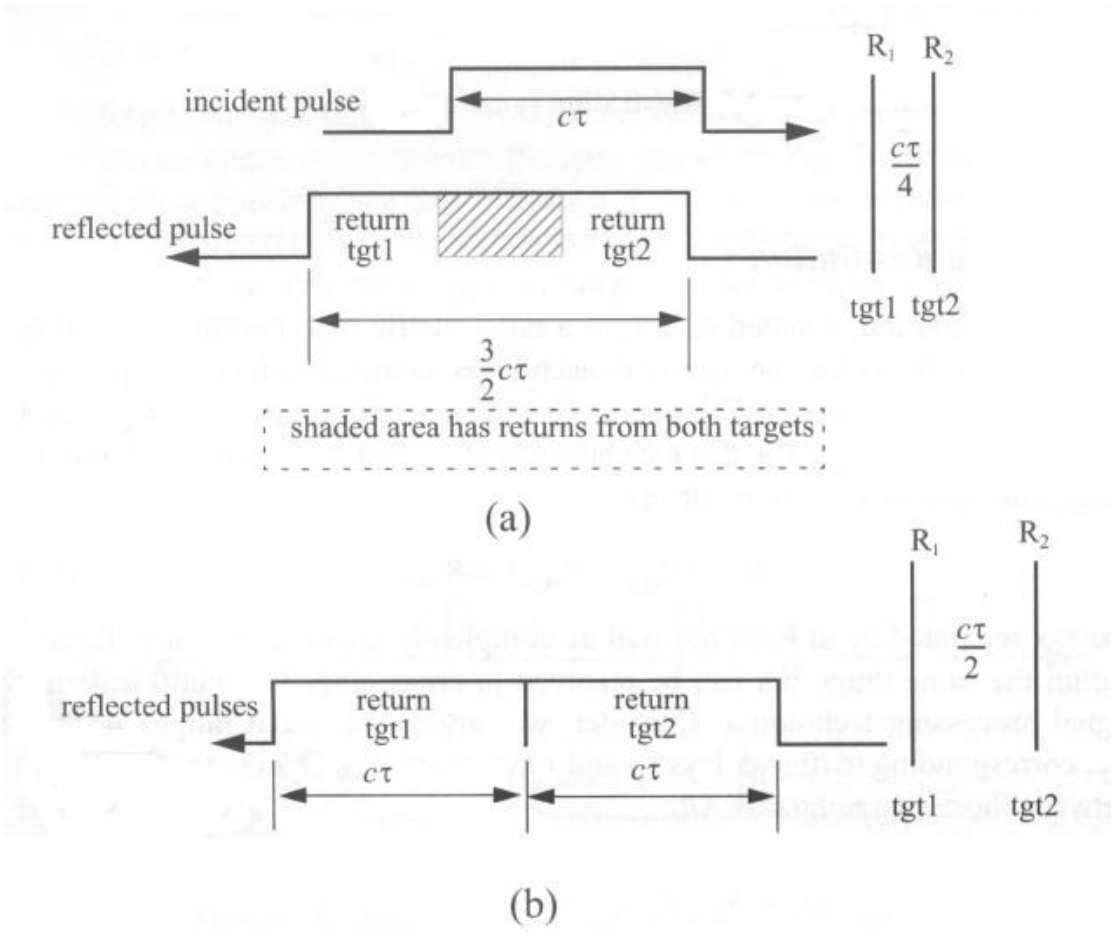

Figure 3- 9: (a) Two unresolved targets. (b) Two resolved targets.

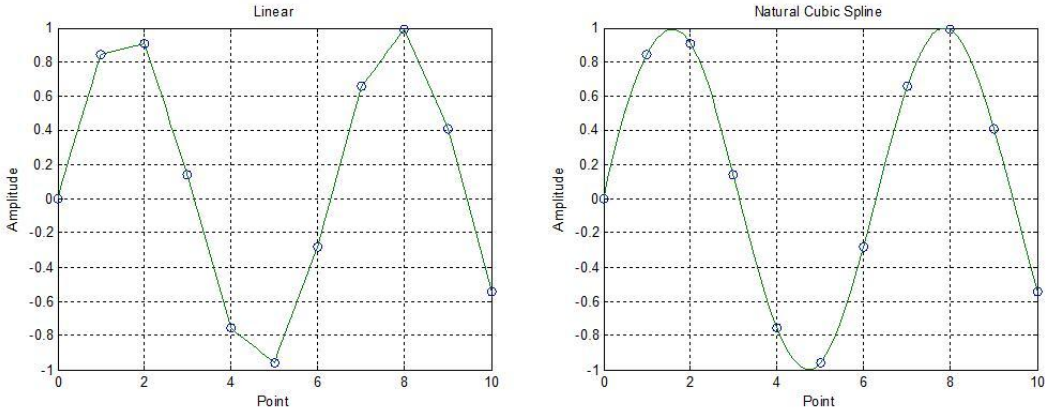

Figure 4- 1: Linear Interpolation and Natural Cubic Spline Interpolation.

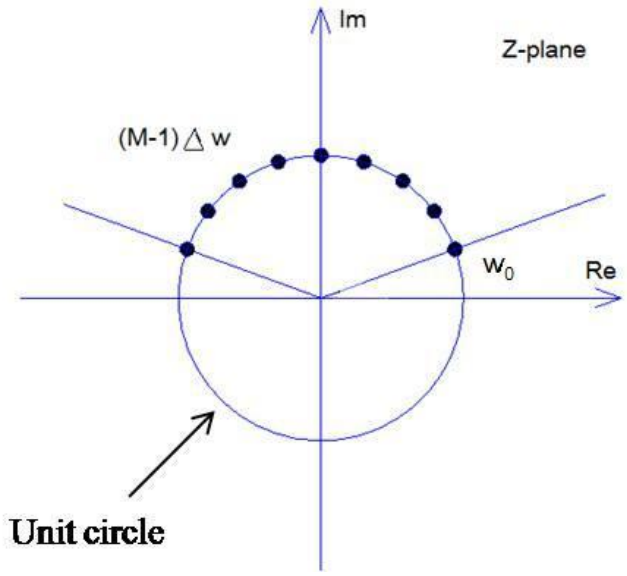

Figure 4- 2: Frequency Samples for Chirp-Z Transform Algorithm.

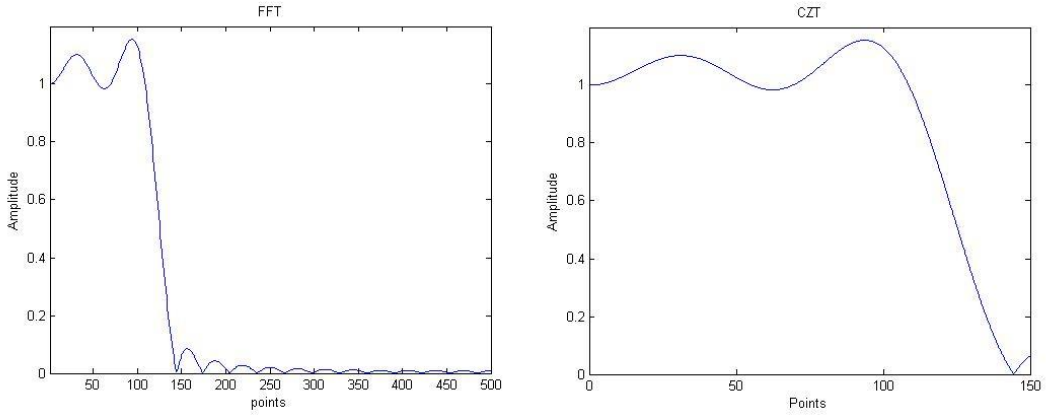

Figure 4- 3: Chirp-Z Transform Result.

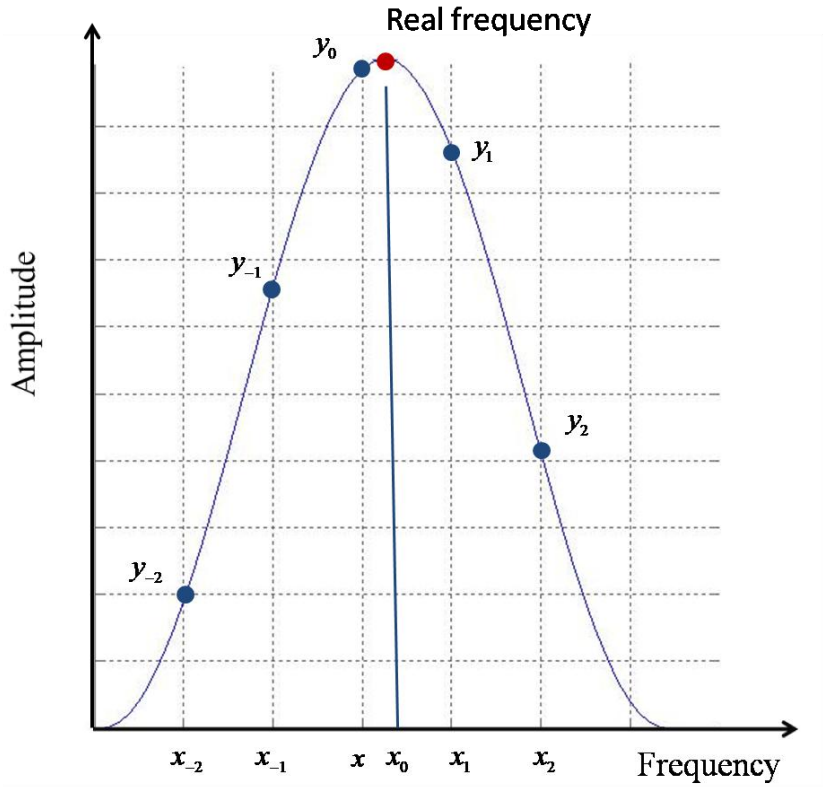

Figure 4- 4: Hanning Window Spectrum Frequency Calibration.

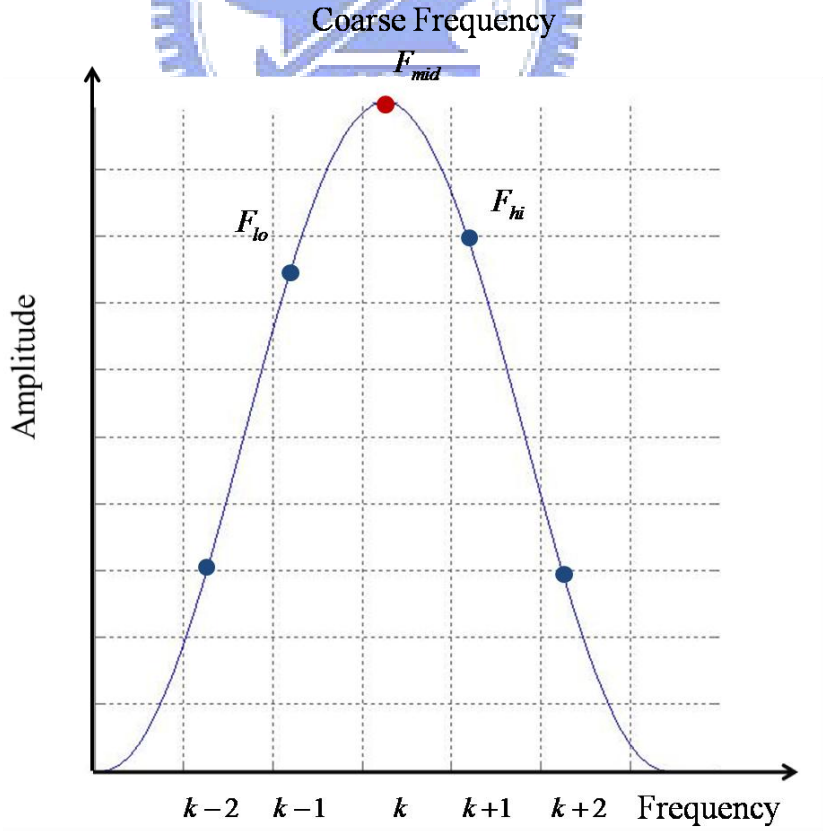

Figure 4- 5: Gradient Search method Coarse Frequency from FFT.

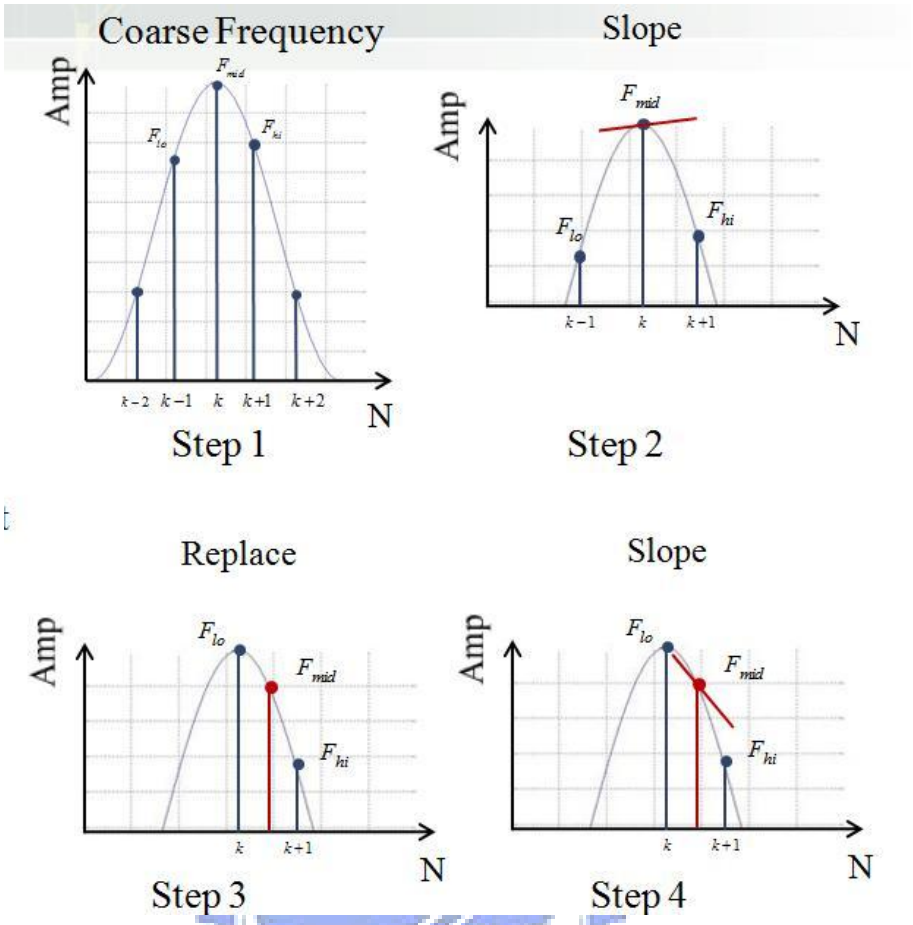

Figure 4- 6: Gradient Search Method Measure Slope.

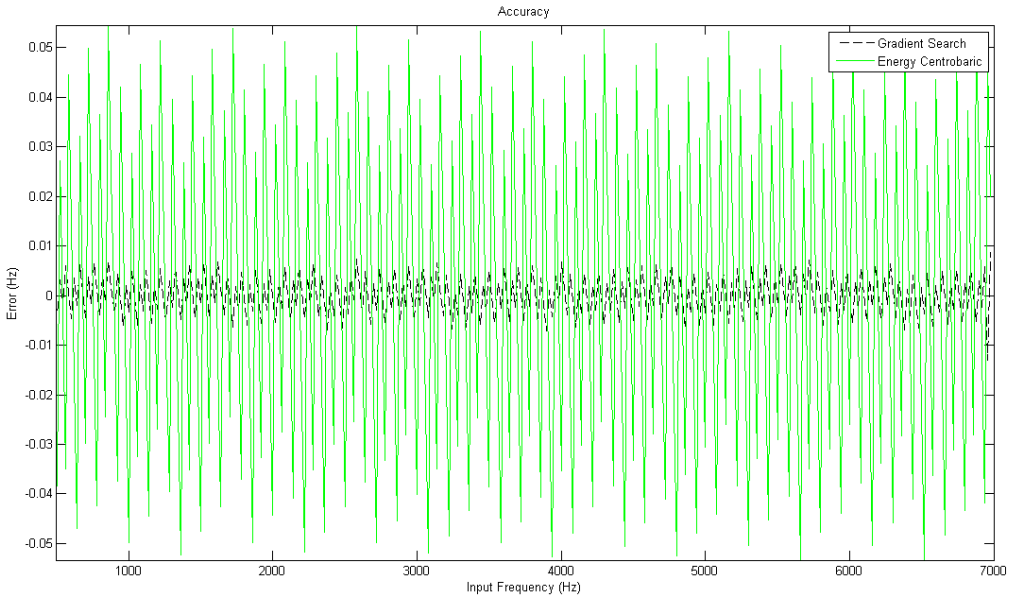

Figure 5- 1: Simulation Results of Gradient Search Method and Energy Centrobaric Method.

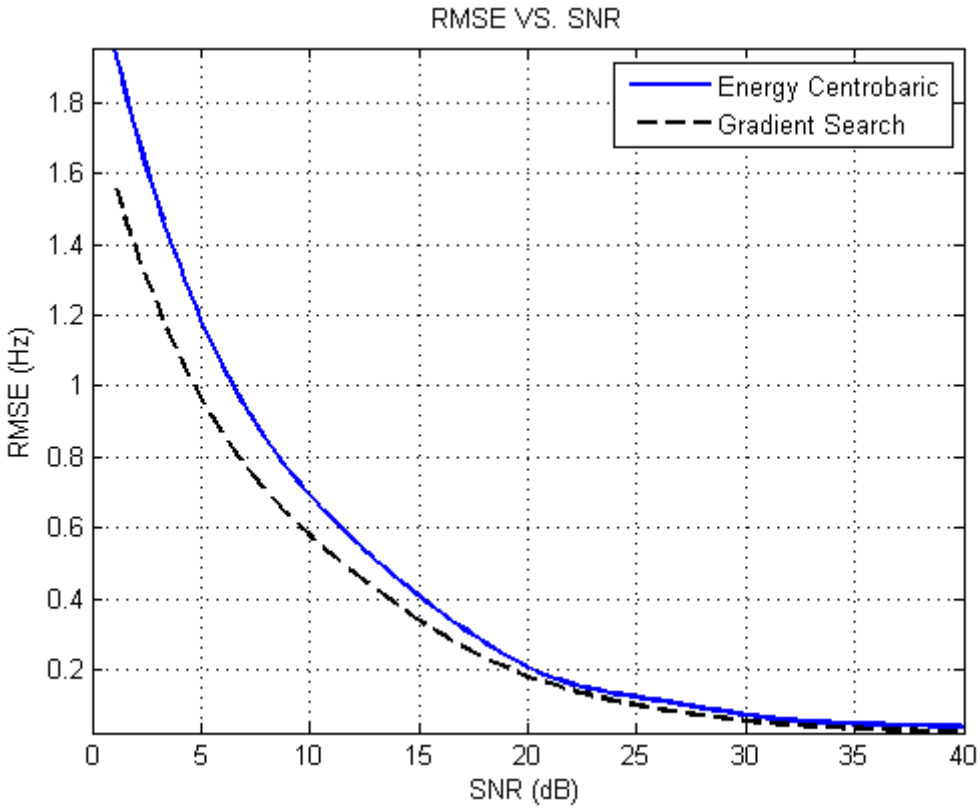

Figure 5- 2: Add White Noise RMSE VS. SNR .

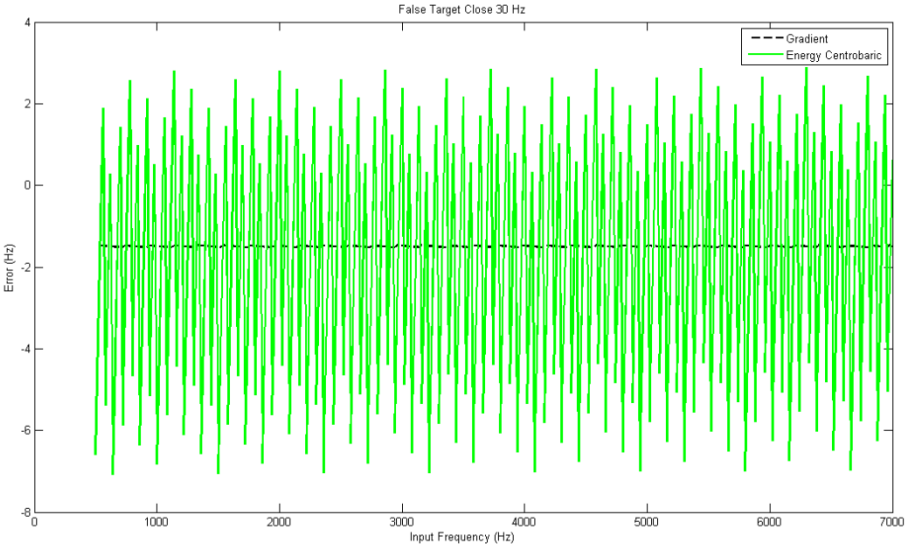

Figure 5- 3: False Target Affect Frequency Error.

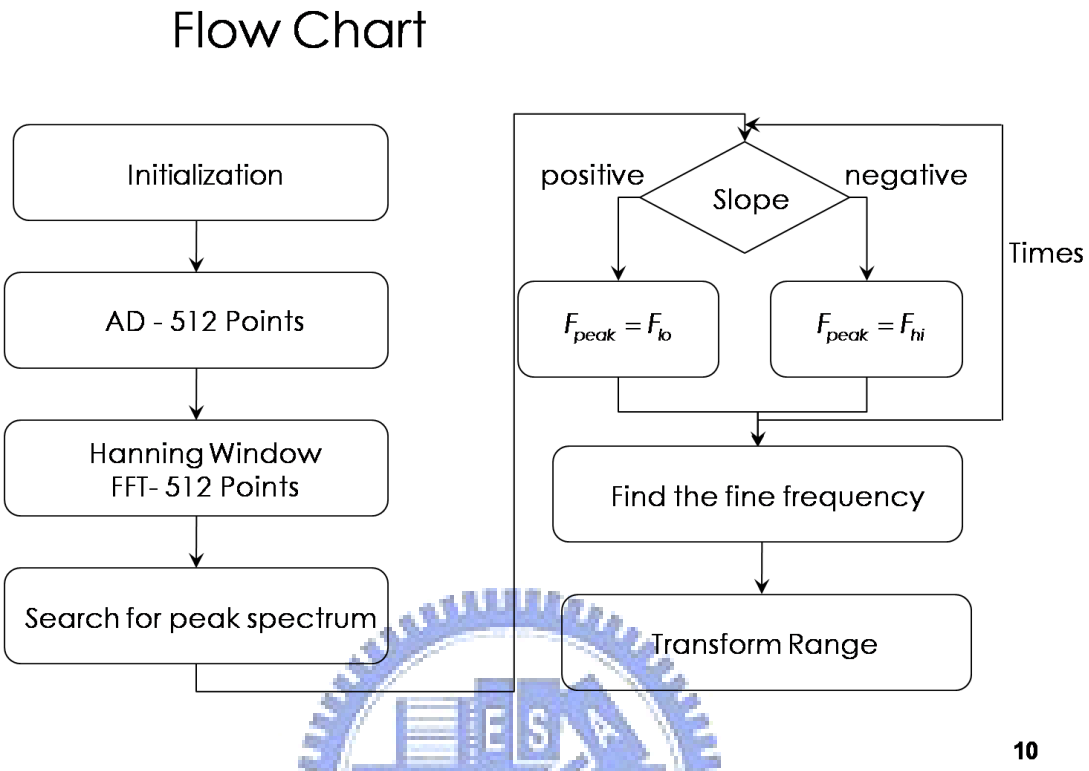

Figure 5- 4: Flow Chart of the dsPIC33F MCU.

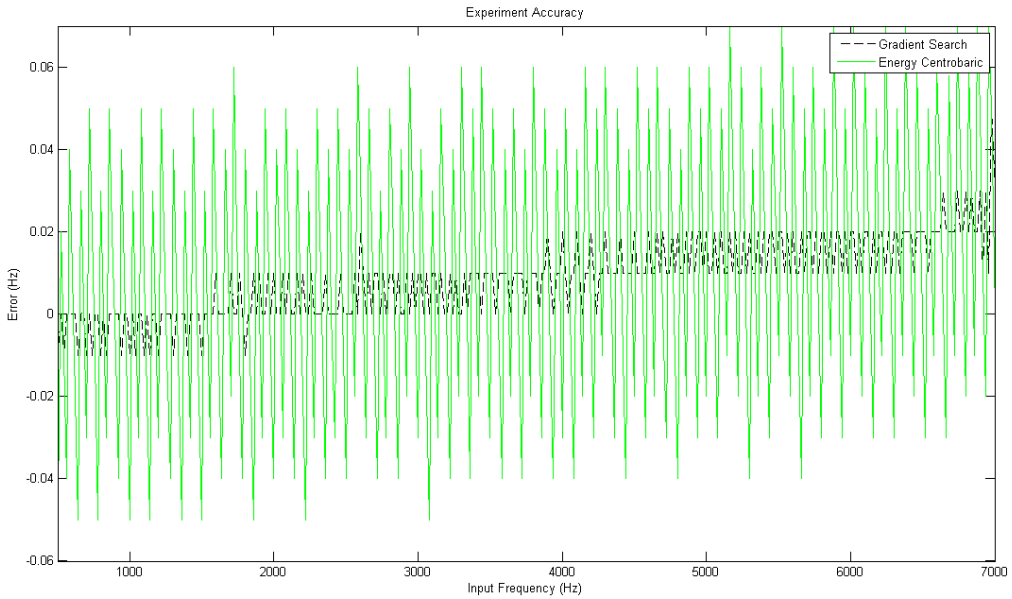

Figure 5- 5: Experiment with Function Generator.